Journal of Catalysis **181,** 16–27 (1999)
Article ID jcat.1998.2282, available online at http://www.idealibrary.com on IDEAL®

The Conversion of 1-Propanamine on Copper-Containing MFI and BEA Zeolites Prepared by Aqueous and Vapor Ion-Exchange

Trent F. Guidry and Geoffrey L. Price[1]

Louisiana State University, Department of Chemical Engineering, Baton Rouge, Louisiana 70803

Received May 11, 1998; revised September 15, 1998; accepted September 18, 1998

A process has been developed for exchanging one Cu atom per ion exchange site in an MFI zeolite. The material is synthesized by reaction of the acidic zeolite with CuCl vapor, followed by oxidation with oxygen, and conversion of the Cu^{2+} species to copper hydroxyl ions and copper hydroxyl dimers by reaction of the oxidized material with water upon exposure to humid air. This material, a similarly prepared BEA material, and copper-containing MFI and BEA zeolites prepared by conventional aqueous ion-exchange have been comparatively investigated for the conversion of 1-propanamine. Reaction products include C_6 products such as dipropanamine and 1-propanamine, N-(1-propylidene). A bifunctional acid/metal reaction pathway is proposed to account for the observed products.

INTRODUCTION

Copper-containing MFI[2] zeolites prepared by reductive solid-state ion-exchange (1) and CuCl vapor ion-exchange (2) have been shown to be active for the conversion of 1-propanamine to C_6 imines and nitriles. Previous investigations suggested that under reaction conditions, the reactant reduces the zeolitic copper cations to the metal which results in a concurrent restoration of zeolitic protons. The conversion of 1-propanamine to dipropanamine, which appears in the reaction products with the C_6 imine and nitriles, was proposed to occur over the zeolite acid sites followed by selective dehydrogenation of dipropanamine by removal of the hydrogen atoms on the dispersed copper metal to yield the imine (2).

In this communication, the Cu-MFI catalyst prepared by CuCl vapor ion-exchange has been characterized by X-ray diffraction, IR analysis of the OH stretch region, IR analysis of the CO absorption band region after CO adsorption, and hydrogen consumption and weight loss during temperature-programmed reduction using hydrogen. Experimental evidence is presented suggesting that in this material nearly all of the zeolite ion-exchanged sites are occupied by $[Cu(OH)]^+$ ions. The close proximity of these ions induces the formation of hydroxyl bridges that have previously been reported in "excessively" exchanged mordenite (3, 4) but do not appear to have been reported for copper exchanged MFI. Heating this material to 773 K in He is shown to cause the reduction of these ions to zeolite-coordinated Cu^+ ions.

The conversion of 1-propanamine has also been investigated over copper exchanged MFI prepared by aqueous ion-exchange and over copper-containing beta zeolite (which we refer to as "BEA") prepared by conventional aqueous ion-exchange and CuCl vapor ion-exchange. For both zeolite structures, the amount of copper introduced by CuCl vapor ion-exchange is theoretically twice as great as that introduced by aqueous ion-exchange. The conversion of 1-propanamine to 1-propanamine, N-(1-propylidene) (a C_6 imine) is shown to increase with copper loading, which is consistent with the dehydrogenation reactions occurring over these sites.

EXPERIMENTAL

Catalyst Preparation

The base zeolites used for ion-exchange were the acidic forms of MFI (Valfor CBV-3020) and BEA (Valfor CP-811BL-25) zeolites supplied by PQ Corporation. Adsorption/desorption of 1-propanamine from the materials (1, 5, 6) indicated a proton concentration of 0.077 and 0.098 moles of protons/100 grams of MFI and BEA zeolite, respectively. Na-MFI was made by mixing 11 g of the H-MFI with 0.33 g of NaOH dissolved in 250 ml of DDI water for 1 h. This solution was then filtered and washed three times with 100 ml of DDI water. Na-BEA was prepared similarly using 0.444 g of NaOH. An aqueous ion-exchanged MFI, referred to hereafter as Cu-MFI/AIE, was prepared by exchanging the Na-MFI material from above with 2.2 g of $CuCl_2$ dissolved in 100 ml of distilled, deionized (DDI) water at room temperature for 16 h. This material was then filtered, rinsed three times with 100 ml of DDI water and

[1] To whom correspondence should be sent.

[2] MFI is the International Zeolite Association's designation for the framework structure that is often referred to as ZSM-5 zeolite.

0021-9517/99 $30.00

dried in air at 373 K for 24 h. An aqueous ion-exchange BEA, referred to hereafter as Cu-BEA/AIE, was prepared by a procedure similar to the MFI material using 3 g of $CuCl_2$ dissolved in 100 ml DDI water.

Copper-containing MFI and BEA materials prepared by vapor ion-exchange, referred to as Cu-MFI/VIE and Cu-BEA/VIE, respectively, were made by first spreading 5 g of the acidic zeolite on a 28.5 cm × 5.75 cm rectangular ceramic boat. 1 g of CuCl was spread along a 28.5 cm × 1.5 cm rectangular ceramic boat which was placed 1.5 cm above the boat containing the zeolite bed. This "double-decker" ceramic boat was placed in a 7-cm ID and 100-cm long quartz tube inside a three-zone Lindberg/BlueM Furnace. The sample was dried in 200 cc/min Ar at 323 K for 2 h and then heated to 973 K at 5 K/min and held at that temperature for 6 h. Due to the disproportionation reaction of 2 Cu^+ to Cu^0 and Cu^{2+} in the presence of water adsorbed by the zeolite from humid air, prior to removal from the furnace, the Cu^+-MFI material must be converted to a different form which can later be restored to Cu^+-MFI. We have determined that the oxidized material can be converted back to the Cu^+-MFI material by either thermal reduction or partial hydrogen reduction. To perform the oxidation, the sample was cooled to 373 K, the gas flow was switched to 50 cc/min O_2, and the sample was allowed to oxidize for 5 h. The sample was cooled to room temperature in oxygen prior to exposure to air, and it is this final oxidized sample that we refer to with the "VIE" appendage.

The VIE and AIE materials were analyzed for copper content after preparation. Copper was extracted from samples of each material by three repetitions of boiling to dryness in aqua regia, followed by a wash in hot, dilute aqueous HCl. The zeolite was then filtered off the aqueous HCl, and the filtrate was analyzed for copper content using ICP. The results are given in Table 1.

A physical mixture of Cu_2O and H-MFI, referred to as Cu_2O/H-MFI, was made by mixing 0.0532 g of Cu_2O with 1 g of H-MFI in a mortar and pestle for 5 min. These samples were made immediately prior to the experiments in which they were used.

Catalytic Reactor Studies

Catalytic reactor experiments were performed at constant temperature in a gradientless recirculating batch reactor system described elsewhere (7). The catalyst was placed between two plugs of quartz wool in a quartz reactor. The circulation loop was equipped with a magnetically operated piston pump and check valve arrangement. The entire system had a volume of 720 cm^3 which could be evacuated with a rotary vacuum pump prior to runs and the system pressure was monitored with diaphragm-type pressure gauges. For these experiments, 100 mg of catalyst was heated under vacuum from 313 K to 773 K at 10 K/min and held for 30 min. The reactor was then cooled to 573 K and filled with 1.33 bar He. The circulation loop was filled with 0.0666 bar 1-propanamine and 1.266 bar He. The reaction was started by diverting the circulating mixture through the catalyst bed.

TABLE 1

Copper Content of Catalysts Measured by ICP

Catalyst	Grams Cu per 100 g zeolite	Moles of framework-Al per 100 g zeolite	Moles of Cu per mole of framework-Al
Cu-MFI/AIE	2.0	0.077	0.41
Cu-MFI/VIE	4.9	0.077	1.00
Cu-BEA/AIE	1.8	0.098	0.29
Cu-BEA/VIE	3.7	0.098	0.60

Samples were withdrawn periodically through a traced line to an evacuated loop on a gas sampling valve. The GC was an HP5890II equipped with a 50-m PONA capillary column and FID detector. Identification of products was done by performing preliminary experiments in the reactor but using a HP 5972 Series Mass Selective Detector instead of the FID. The absolute areas from the FID detector were used to determine the conversion of 1-propanamine and the partial pressure of the products formed.

Microbalance Experiments

Microbalance TA experiments were performed on a Perkin-Elmer TGA7 interfaced to a PC. A 12–18-mg portion of sample was placed on the Pt microbalance pan. A 50 cc/min He stream continuously purged the microbalance mechanism and mixed with a 50 cc/min reagent gas stream that could be varied in composition. The weight curves obtained could also be numerically differentiated by the computer with respect to time. The reagent gas stream could also be saturated with 1-propanamine by diverting it through a room temperature saturator.

Microbalance reduction experiments were performed by heating the sample in 100 cc/min He from 313 K to either 473 K or 773 K at 10 K/min and were held at the final temperature for 30 min. The samples were then cooled to 323 K in He and a temperature program at 10 K/min to 923 K was started as the gas flow was switched to 5 cc/min H_2 in 95 cc/min He. One Cu-MFI/VIE was pretreated to 773 K as above and then cooled to 323 K. This sample was heated in 5 cc/min CO and 95 cc/min He to 773 K at 10 K/min. When the sample temperature reached 773 K, the gas flow was switched to 100 cc/min He and the sample was held at this temperature for 30 min. This sample was then cooled and reduced as above.

Bulk CuO, Cu_2O, $CuCl_2$, and CuCl samples were also reduced after drying in 100 cc/min He at 323 K for 15 min by heating the samples from 323 K to 923 K at 10 K/min in 5 cc/min H_2 and 95 cc/min He. Cu_2O was also similarly reduced in 5 cc/min CO and 95 cc/min He.

Microbalance CO adsorption experiments were performed by heating the sample in 100 cc/min He from 313 K to either 473 K or 773 K at 10 K/min and were held at the final temperature for 30 min. The samples were then cooled to 323 K in He, held at 323 K for 1 min in 100 cc/min He while data gathering began, then the gas flow was switched to 5 cc/min CO in 95 cc/min He for 9 min, and then the gas flow was then switched back to 100 cc/min He to purge weakly bound CO. Some of the samples were partially reduced after thermal pretreatment and prior to CO adsorption by heating the samples from 323 K to the final reduction temperature, specified later, in 5 cc/min H_2 and 95 cc/min He and holding at that temperature for 10 min. The samples were then cooled and purged in pure He prior to performing CO adsorption experiments.

Temperature Programmed Reduction (TPR) Experiments

A Carle Analytical Gas Chromatograph 111 H Series S was reconfigured to measure hydrogen consumption and was interfaced to a PC for TPR experiments. In the basic TPR configuration, a reactant stream of hydrogen and argon flowed through a quartz reactor which contained the catalyst sample then to a palladium hydrogen transfer cell, where the hydrogen in the reactant stream was transferred to a pure Ar stream flowing at 30 cc/min. The later stream is then analyzed by a thermistor detector, so that when hydrogen is removed by reaction from the stream flowing over the catalyst sample, an imbalance in the thermistor detector is recorded. The areas of the hydrogen consumption peaks were numerically integrated and quantitative measure was made by comparison with the measured area of a 100-mg sample of 5% bulk CuO ball milled with H-MFI that was dried at 473 K.

A series of experiments were performed on this apparatus using 100 mg of all samples except Cu-BEA/AIE, for which a 200-mg sample was used. The samples were pretreated by heating in 57 cc/min Ar from 303 K to either 473 K or 773 K at 10 K/min and held at the final temperature for 30 min. The samples were then cooled to 303 K in Ar. The gas flow was then switched to 3 cc/min H_2 and 57 cc/min Ar and heated from 303 K to 923 K at 10 K/min.

X-Ray Diffraction (XRD) Experiments

X-ray diffraction data were collected with a Scintag PAD-V diffractometer equipped with a Cu Kα radiation source. Data were collected using step scans of 0.02° from 3° to 60° at 1°/min.

Infra-Red Spectroscopy (IR) Experiments

IR spectra were taken in the transmittance mode using an IBM IR-30 FTIR. The zeolites were pressed into self supporting wafers, 6.4 mg/cm^2, which were loaded into a controlled atmosphere quartz IR cell with KBr windows. The samples were pretreated by heating in a flow of 50 cc/min He from 303 K to either 473 K or 773 K at 10 K/min, held at the final temperature for 30 min, and then cooled to 323 K. Spectra of samples with adsorbed CO were taken after exposure of the sample to 2.6 cc/min CO and 50 cc/min He for 45 min then desorbed in pure He for 10 min at 323 K. Some of the samples were partially reduced after thermal pretreatment and prior to CO adsorption by heating the samples from 323 K to the final reduction temperature, specified in each experiment, in 2.6 cc/min H_2 and 50 cc/min He and held at the final temperature for 10 min.

RESULTS

Reactor Experiments

The conversion of 1-propanamine as a function of time over a set of catalytic materials is shown in Fig. 1. The acidic BEA zeolite is more active than the acidic MFI material. Addition of copper by aqueous ion-exchange increases the rate of conversion of 1-propanamine for both the MFI and BEA zeolites and the rate of conversion is further increased by addition of copper by CuCl vapor ion-exchange. The major products observed are dipropanamine and 1-propanamine, N-(1-propylidene) and their partial pressures as a function of time as shown in Figs. 2 and 3, respectively. For both H-MFI and H-BEA, the net rate of formation of dipropanamine is positive throughout the experiment. The net rate of formation of dipropanamine over both the Cu-MFI/AIE and Cu-BEA/AIE materials is zero or slightly negative after approximately 4 ks. After approximately 2 ks, a maximum observed in the partial pressure curve indicates that the rate of dipropanamine conversion exceeds that of its formation for both the Cu-MFI/VIE

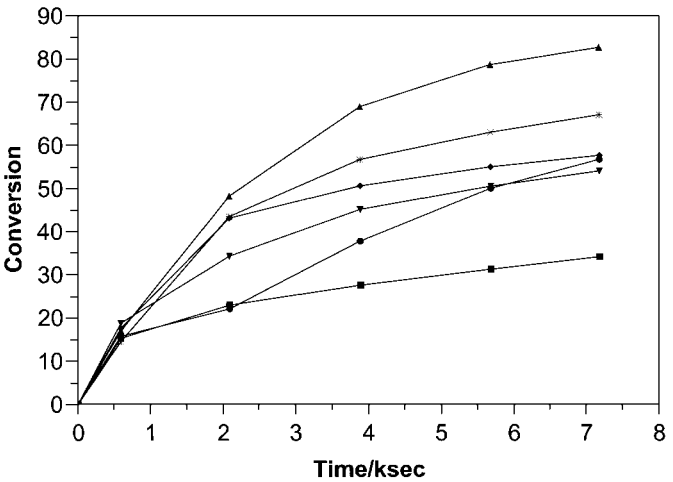

FIG. 1. Conversion of 1-propanamine at 573 K over 0.1 g catalyst: ■, H-MFI; ●, Cu-MFI/AIE; ▲, Cu-MFI/VIE; ▼, H-BEA; ◆, Cu-BEA/AIE; ✳, Cu-BEA/VIE.

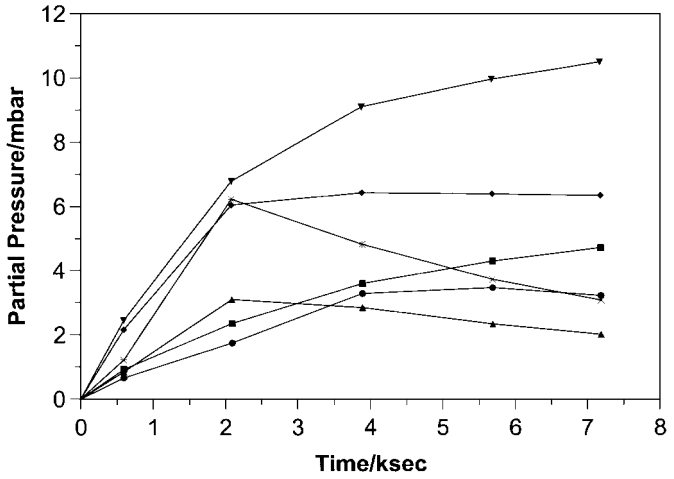

FIG. 2. Partial pressure of dipropanamine from the 1-propanamine reaction at 573 K over 0.1 g catalyst: ■, H-MFI; ●, Cu-MFI/AIE; ▲, Cu-MFI/VIE; ▼, H-BEA; ◆, Cu-BEA/AIE; ❋, Cu-BEA/VIE.

and Cu-BEA/VIE materials. Figure 3 indicates that the amount of 1-propanamine, N-(1-propylidene) formed over the CuCl vapor ion-exchange materials is greater than that over the aqueous ion-exchanged materials, which are in turn greater than that over the acidic zeolites. The product distribution for all significant products of 1-propanamine conversion at various times over Cu-MFI/VIE, one of the most active materials, is shown in Table 2.

X-Ray Diffraction

Comparison of the X-ray diffraction patterns of the catalytic materials with that of the pure CuO, Cu_2O, CuCl, and $CuCl_2$ indicated the absence of extracrystalline CuO, Cu_2O,

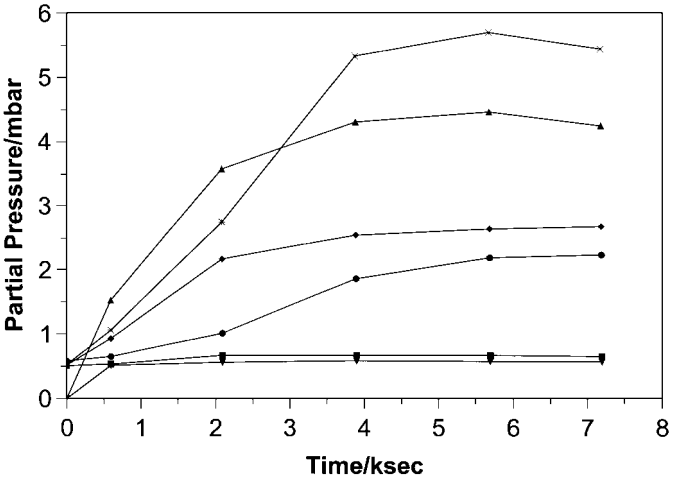

FIG. 3. Partial pressure of 1-propanamine, N-(1-propylidene) from the 1-propanamine reaction at 573 K over 0.1 g catalyst: ■, H-MFI; ●, Cu-MFI/AIE; ▲, Cu-MFI/VIE; ▼, H-BEA; ◆, Cu-BEA/AIE; ❋, Cu-BEA/VIE.

TABLE 2

Distribution of Products from 1-Propanamine Conversion over 0.100 g Cu-MFI/VIE at 573 K

Time (ks)	0.6	2.1	3.9	7.2
Conversion (based on area of 1-PA)	16.9	48.2	68.9	82.5
Product weight %				
Dipropanamine	30.4	42.5	34.0	22.3
1-Propanamine, N-(1-propylidene)	69.6	48.3	53.7	51.6
Propanitrile	—	—	2.7	9.3
4-Methylpentanitrile	—	—	—	1.5
Tripropylamine	—	—	—	5.2
Dipropanamine, N-(1-propylidene)	—	9.2	9.6	9.1

and $CuCl_2$ in all of the samples, except that nonzeolitic peaks at 16.0° and 32.3° were observed for the Cu-MFI/VIE and Cu-BEA/VIE, which are consistent with the presence of extraframework CuCl. Some loss of signal intensity was observed for the Cu-BEA/AIE and Cu-BEA/VIE relative to that of the H-BEA material, suggesting that some loss of crystallinity occurs during the copper exchange procedure.

Temperature Programmed Reduction (TPR)

We have found that the oxidation state of copper is a function of the temperature that the material is pretreated to under an inert atmosphere or vacuum prior to use in the TPR or in the catalytic reactor. Therefore, an appendage "XXXK" is added to the name of each material to indicate the temperature (XXX) that the material has been pretreated under vacuum or in an inert gas for 0.5 h in all cases. The TPR results for the Cu-MFI/AIE, Cu-MFI/VIE, and H-MFI materials pretreated to 473 K and 773 K are compared in Fig. 4. If the copper content was equivalent to 1 Cu/framework Al, and if the copper exists as Cu^{2+} ions, we would expect that 2 H atoms per copper or per framework Al are required to complete the reduction. For Cu-MFI/VIE the framework Al content is 0.077 mol/100 g, so the Cu^{2+} material would require 0.154 moles H atoms for complete reduction. Since both quantities are useful for comparative purposes, in appropriate places, we give the hydrogen consumption in moles per 100 grams of zeolite and, in parenthesis, we give the equivalent H atoms consumed per framework Al. As expected, the H-MFI/473 K does not show any hydrogen reduction peaks. The Cu-MFI/VIE/473 K shows two well-defined reduction peaks. The amount of hydrogen consumed corresponds to approximately 0.077 mol H/100 g (1.0 H/framework Al) and 0.085 mol H/100 g (1.1 H/framework Al) for the first and second peaks, respectively, for a total of 0.162 mol H/100 g (2.1 H/framework Al). A shoulder on the first peak at 463 K is observable. The Cu-MFI/VIE/773 K shows two distinct but nonresolvable peaks. The hydrogen consumed

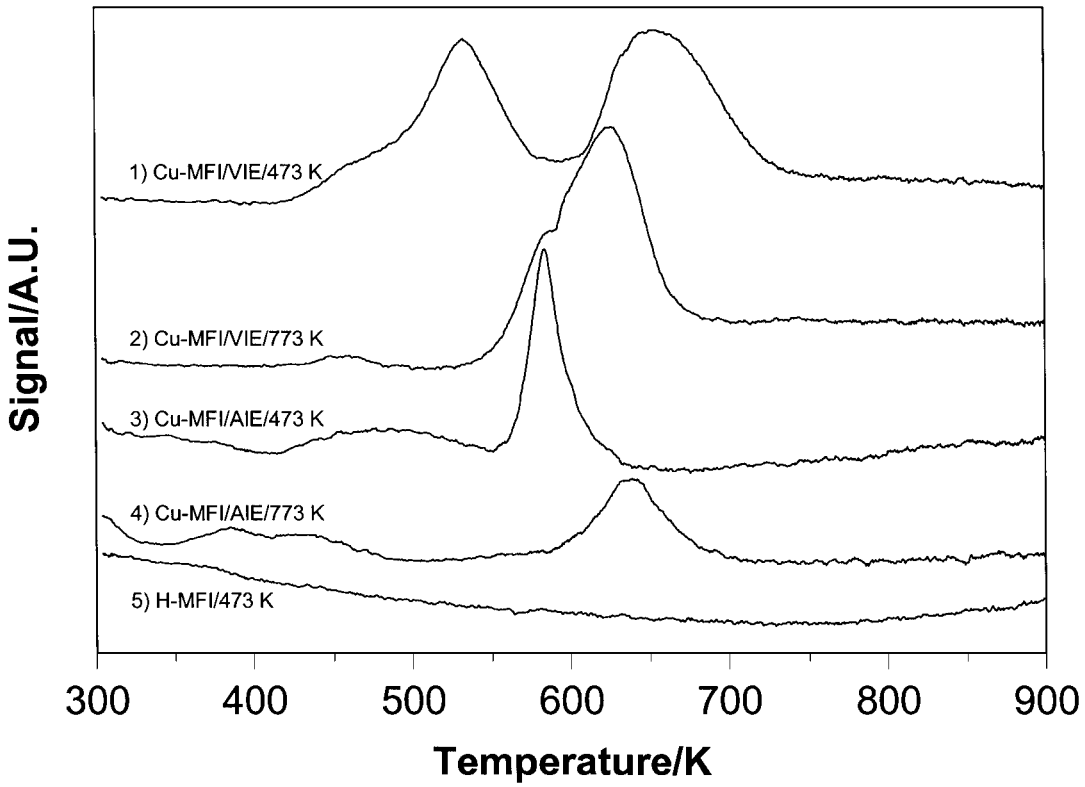

FIG. 4. TPR Results: (1) Cu-MFI/VIE/473 K; (2) Cu-MFI/VIE/773 K; (3) Cu-MFI/AIE/473 K; (4) Cu-MFI/AIE/773 K; (5) H-MFI/473 K.

during this experiment corresponded to approximately 0.106 mol H/100 g (1.4 H/framework Al), suggesting that thermal reduction of copper partially occurred, since the total reduction capacity has fallen from 0.162 moles to 0.106 moles. Cu-MFI/AIE/473 K also shows two reduction peaks. The amount of hydrogen consumed corresponds to approximately 0.020 mol H/100 g (0.3 H/framework Al) and 0.044 mol H/100 g (0.6 H/framework Al) for the first and second peaks, respectively. For Cu-MFI/AIE/773 K, a broad low temperature reduction peak, consuming approximately 0.012 mol H/100 g (0.2 H/framework Al), and a more pronounced high temperature peak, consuming approximately 0.034 mol H/100 g (0.4 H/framework Al), is observed. These results indicate that the Cu-MFI/AIE material also undergoes thermal reduction upon heating to 773 K. The thermal reduction of Cu^{2+} ions to Cu^{+} ions in aqueous ion-exchanged zeolites has been observed previously (9–19).

The BEA materials behave similarly to the MFI materials as shown in Fig. 5. Cu-BEA/VIE/473 K possesses two distinct reduction peaks consuming approximately 0.062 mol H/100 g (0.6 H/framework Al) and 0.063 mol H/100 g (0.6 H/framework Al). Cu-BEA/VIE/773 K possesses only one significant peak that consumes 0.056 mol H/100 g (0.6 H/framework Al). Due to the low loadings of copper in Cu-BEA/AIE, twice as much material had to be used to obtain measurable TPR peaks. Cu-BEA/AIE/473 K possesses two peaks with hydrogen consumption corresponding to approximately 0.021 mol H/100 g (0.2 H/framework Al) and 0.030 mol H/100 g (0.3 H/framework Al), while Cu-BEA/AIE/773 K possesses only one peak with a hydrogen consumption of 0.027 mol H/100 g (0.3 H/framework Al).

Microbalance Reduction

Under the conditions employed for copper-zeolite materials, hydrogen reduction of reference samples of the pure copper oxides and chlorides indicated that bulk $CuCl_2$ and CuCl begin to volatilize prior to reduction. Both the CuO and Cu_2O reduce to copper metal with reduction peak maxima at 552 K and 602 K, respectively. Cu_2O also reduces to copper metal in CO with a reduction peak maximum at 545 K.

The microbalance reduction experiments using H_2 compliment the TPR experiments performed above. Even though the reaction which takes place is identical for both experiments, hydrogen consumption by the material is measured by TPR while weight loss from the catalysts is recorded by the microbalance reductions, so that reactions which produce a volatile product such as $Z^{-}[CuOH]^{+} + \frac{1}{2}H_2 \rightarrow Z^{-}Cu^{+} + H_2O$ are recorded by both TPR and microbalance experiments. Experiments which do not result in a volatile product such as $Z^{-}Cu^{2+}Z^{-} + H_2 \rightarrow 2\,Z^{-}H^{+} + Cu^{0}$ have almost no effect on the microbalance reduction

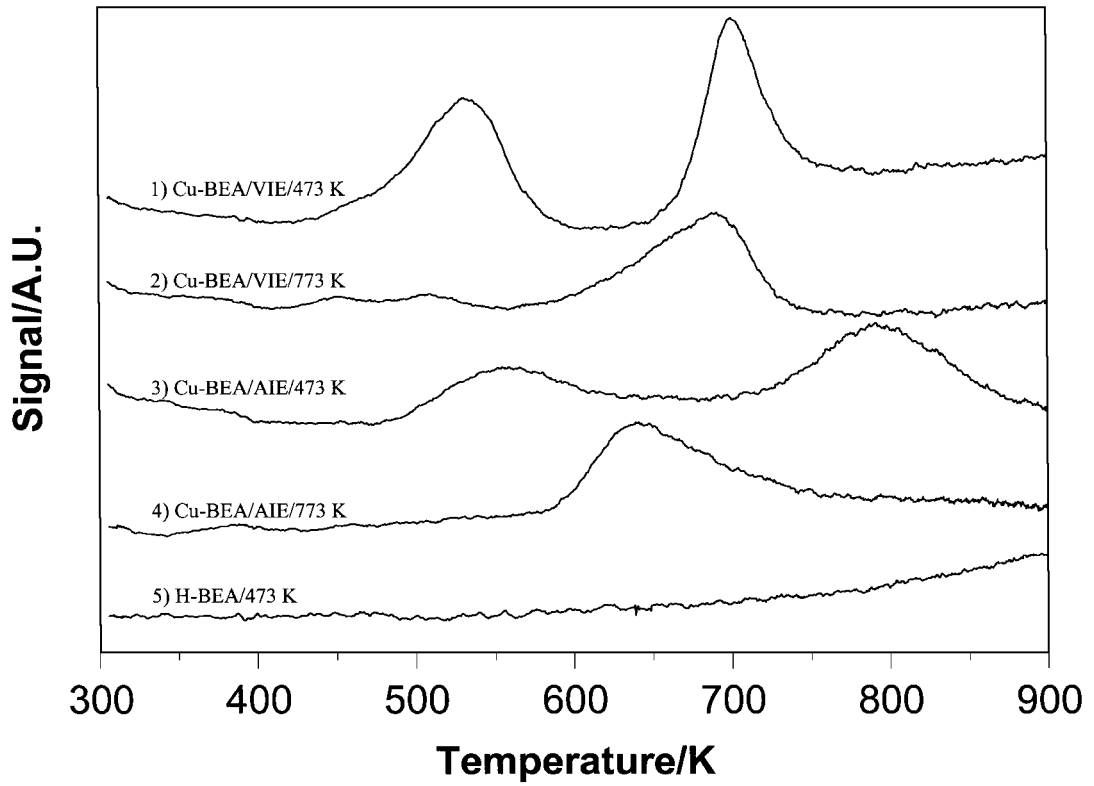

FIG. 5. TPR Results: (1) Cu-BEA/VIE/473 K; (2) Cu-BEA/VIE/773 K; (3) Cu-BEA/AIE/473 K; (4) Cu-BEA/AIE/773 K; (5) H-BEA/473 K.

experiments due to the low molecular weight of H_2, but are easily observed by the TPR apparatus. By comparing the hydrogen consumption, obtained from the TPR, with the weight loss during reduction, from the microbalance, an average molecular weight of the volatile product can be obtained.

The derivative of the microbalance reduction curves for the copper MFI materials are shown in Fig. 6. Cu-MFI/VIE/473 K shows two weight loss peaks, suggesting that both of the TPR peaks for this material (see Fig. 4) correspond to the reduction of copper species possessing extraframework ligands. The weight loss of the first peak corresponds to 1.802 g per 100 g of material, compared to a weight loss of 0.588 g per 100 g of material for the H-MFI/473 K material which is due to further drying above 473 K. The difference between these numbers, 1.214 g/100 g of material, divided by the moles of hydrogen consumed (from TPR measurements) gives a mass to charge ratio of 18.55 for the first peak. A similar calculation for the second peak gives a mass to charge ratio of 16.10. Cu-MFI/VIE/773 K also possesses a weight loss peak which, after subtracting the water content of H-MFI/773 K material, corresponds to 1.351 g/100 g of material. Heating the material to 773 K in CO after the thermal treatment does not significantly change the weight loss peak observed during hydrogen reduction, suggesting that this peak is due to the loss of chlorine rather than oxygen. Assuming that the weight loss is due to chlorine, this corresponds to 0.038 mol/100 g of material. Cu-MFI/AIE/473 K shows three weight loss peaks. The first is in the same temperature region as the first TPR peak in Fig. 4 and the other two are in same region as the second TPR peak. The mass to charge ratios of the first and second TPR peaks correspond to 16.09 and 9.31, respectively. Cu-MFI/AIE/773 K does not possesses any significant weight loss peaks during reduction.

The microbalance reduction curves for the BEA materials are shown in Fig. 7. As with the MFI material, Cu-BEA/VIE/473 K gives two weight loss peaks with mass to charge ratios of 19.51 and 14.40 for the first and second peaks, respectively. Cu-BEA/VIE/773 K has a weight loss peak at the same temperature as Cu-MFI/VIE/773 K. The weight loss of this peak, after subtraction of water loss from the similarly treated H-BEA, corresponds to 0.877 g/100 g of material, or 0.0247 mol/100 g of material, assuming that this weight loss is due to chlorine. Cu-BEA/AIE/473 K shows two weight loss peaks with mass to charge ratios of 17.52 and 19.62 for the first and second peaks, respectively. Cu-BEA/AIE/773 K does not show any significant weight loss peaks.

The CO adsorption results at 323 K are shown in Figs. 8 and 9. Cu-MFI/VIE/773 K experiences the greatest weight gain on exposure to CO. Significant amounts of CO are also adsorbed on the similarly treated Cu-MFI/AIE

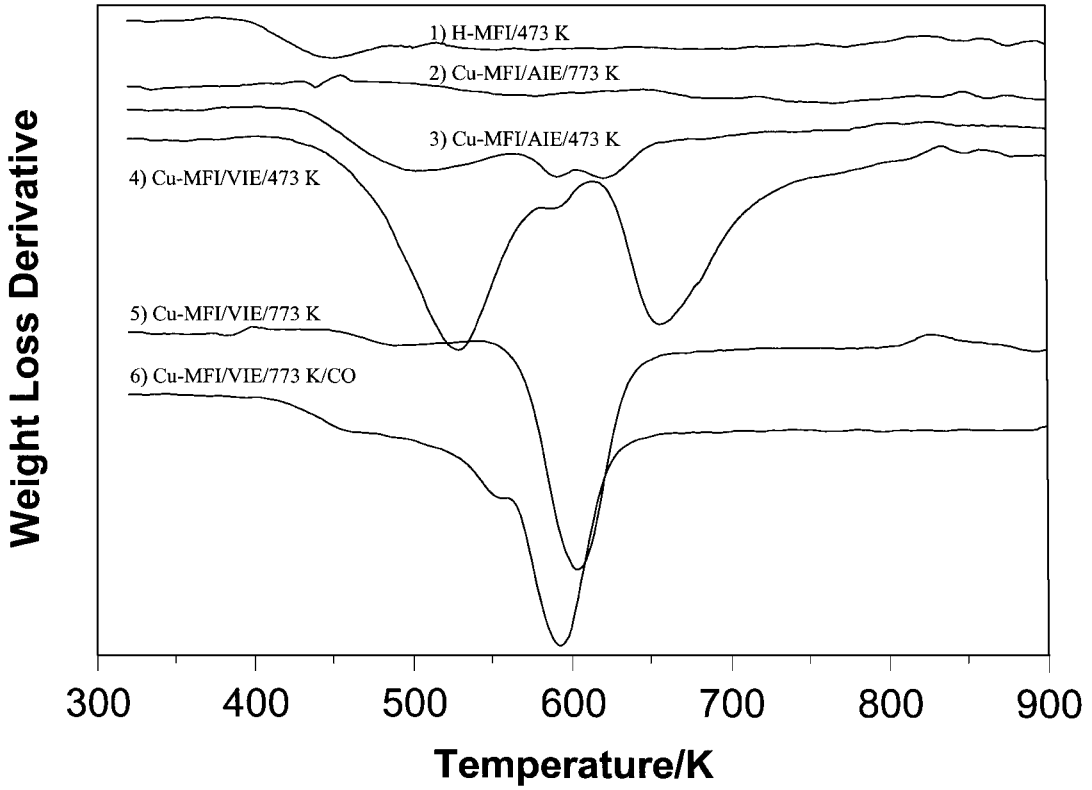

FIG. 6. Microbalance reduction results: (1) H-MFI/473 K; (2) Cu-MFI/AIE/773 K; (3) Cu-MFI/AIE/473 K; (4) Cu-MFI/VIE/473 K; (5) Cu-MFI/VIE/773 K; (6) Cu-MFI/VIE/773 K and then heated to 773 K in CO.

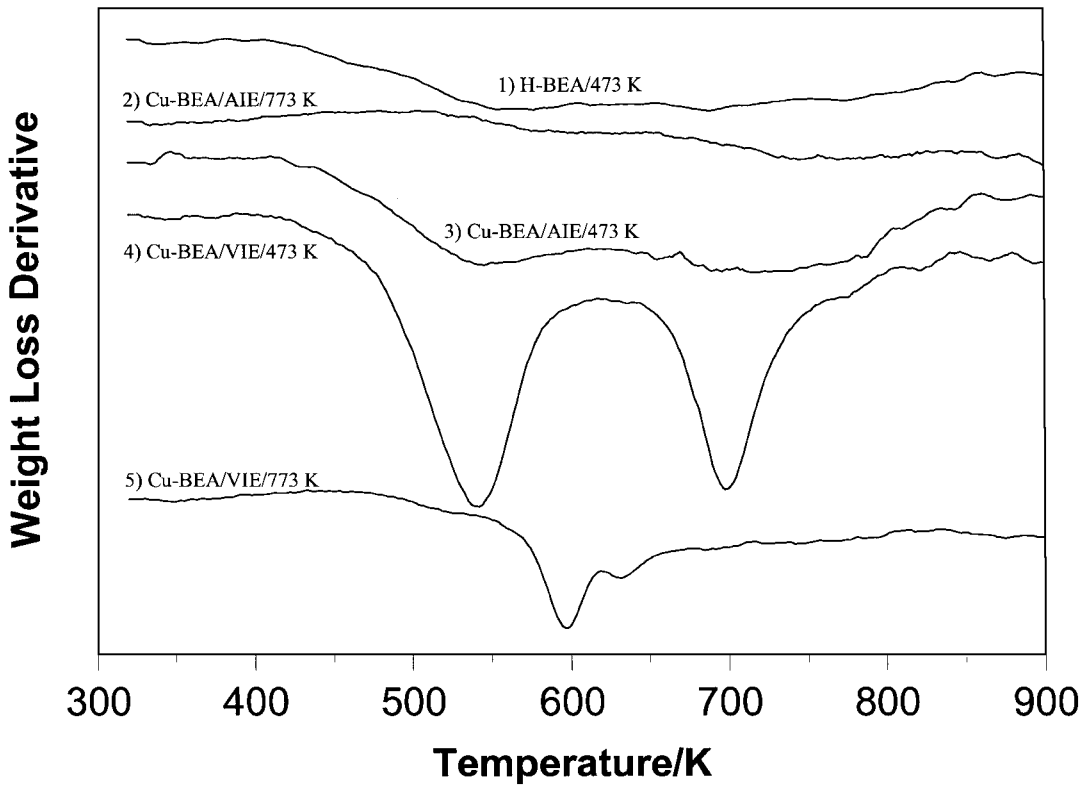

FIG. 7. Microbalance reduction results: (1) H-BEA/473 K; (2) Cu-BEA/AIE/773 K; (3) Cu-BEA/AIE/473 K; (4) Cu-BEA/VIE/473 K; (5) Cu-BEA/VIE/773 K.

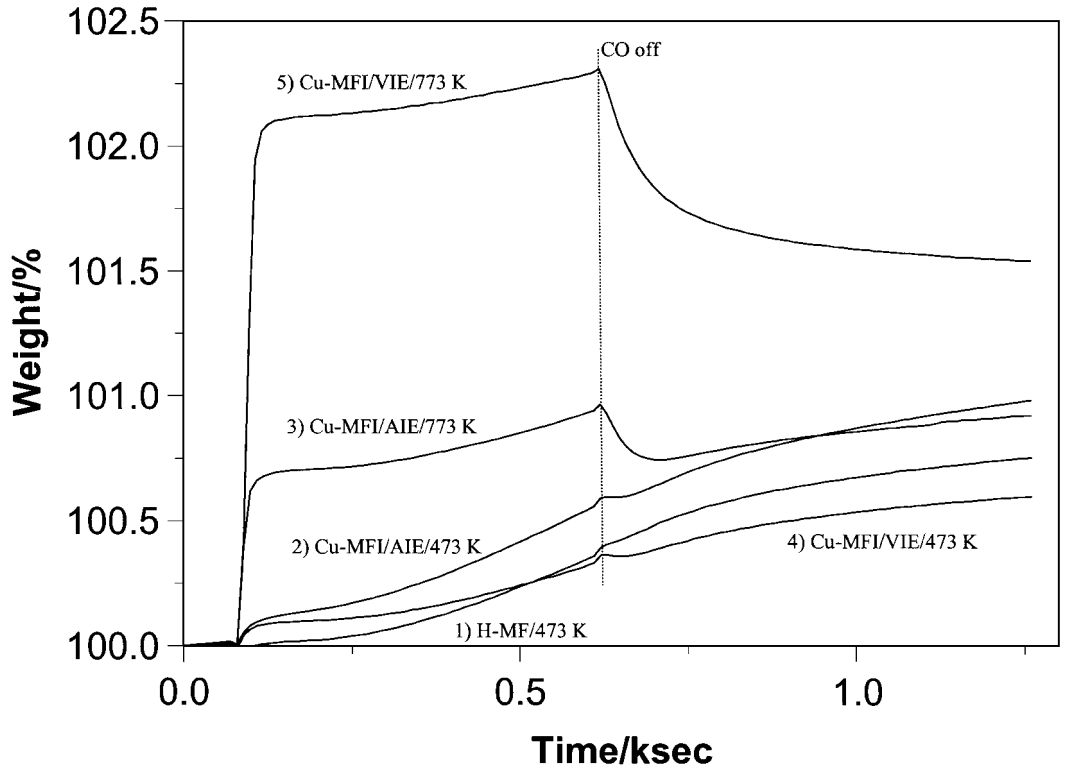

FIG. 8. Microbalance CO adsorption results: (1) H-MFI/473 K; (2) Cu-MFI/AIE/473 K; (3) Cu-MFI/AIE/773 K; (4) Cu-MFI/VIE/473 K; (5) Cu-MFI/VIE/773 K.

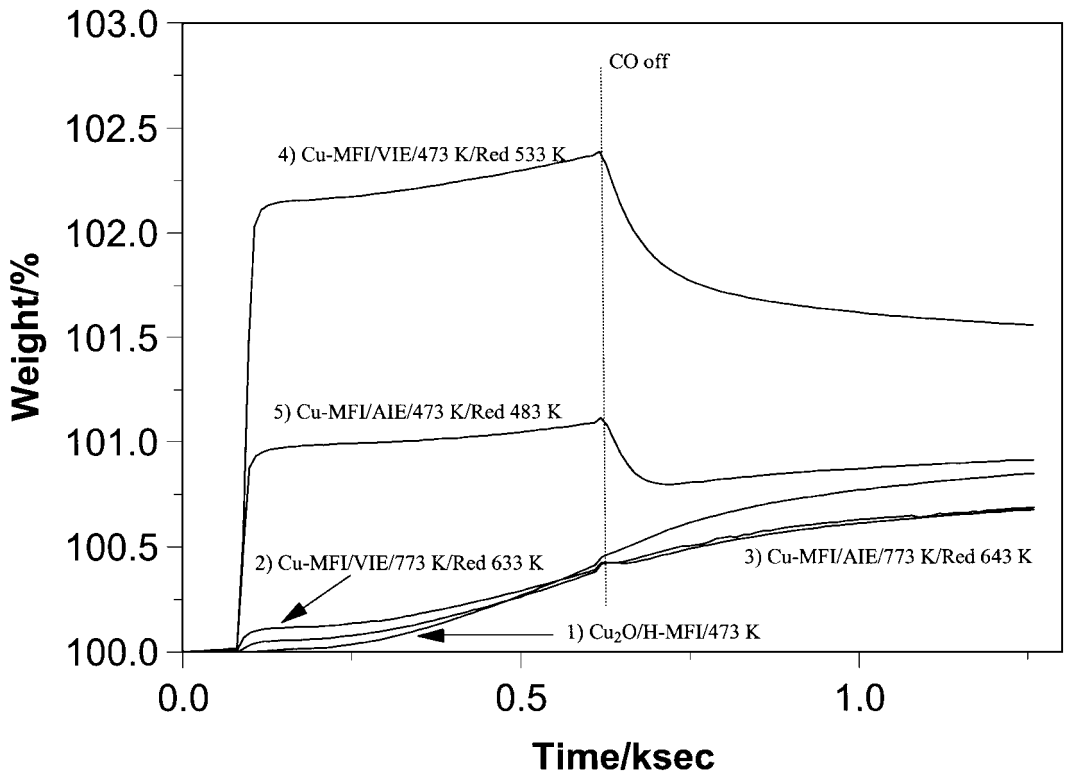

FIG. 9. Microbalance CO adsorption results: (1) Cu_2O/H-MFI/473 K; (2) Cu-MFI/VIE/773 K partially reduced to 633 K; (3) Cu-MFI/AIE/ 773 K partially reduced to 643 K; (4) Cu-MFI/VIE/473 K partially reduced to 533 K; (5) Cu-MFI/AIE/473 K partially reduced to 483 K.

material. Substantially less CO adsorption occurs on the Cu-MFI/VIE/473 K, Cu-MFI/AIE/473 K, and H-MFI/473 K. Partial reduction of the Cu-MFI/VIE/773 K and Cu-MFI/AIE/773 K at 633 K and 643 K, respectively, results in a considerable decrease in the amount of CO adsorbed relative to the unreduced material. (The partial reduction temperatures correspond to the peak maxima in the TPR curves for these two materials.) Partial reduction of Cu-MFI/VIE/473 K and Cu-MFI/AIE/473 K at 533 K and 483 K, respectively, results in a considerable increase in the amount of CO adsorbed, compared to the unreduced materials. (These partial reduction temperatures approximately correspond to the first peak maximum in the TPR curves for these materials.) The Cu_2O/H-MFI physical mixture does not significantly adsorb CO.

Infra-Red (IR)

The IR spectra of the OH stretching region of the materials are shown in Fig. 10. Four important peaks are observable for H-MFI/473 K. The 3738 cm^{-1} band, which is present in all of the samples shown, has been attributed to hydroxyl groups attached to terminal silicon atoms (4, 11, 20–22). The 3610 cm^{-1} has been attributed to stretching of the acidic hydroxyl group in MFI zeolites (22). Two other minor bands at 3694 cm^{-1} and 3661 cm^{-1} are also observed. Previous investigations have assigned bands at 3690 cm^{-1} (21) and 3656 cm^{-1} (11) to vibrations associated with AlOH groups, suggesting that the minor bands are also due to these species. The Na-MFI material dried to 473 K does not possess the 3610 cm^{-1} band, which is consistent with the replacement of all of the zeolitic protons with Na^+ ions. The increase in the IR bands at 3670 cm^{-1} and 3660 cm^{-1} for the Na-MFI are possibly due to hydroxylation of extraframework alumina by NaOH during sodium exchange. The bands between 3590 cm^{-1} and 3575 cm^{-1} may be due to water bound to the sodium ions.

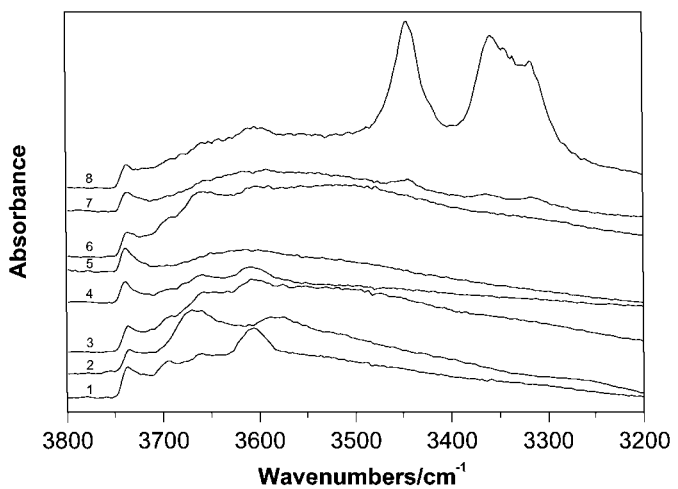

FIG. 10. IR results: (1) H-MFI/473 K; (2) Na-MFI/473 K; (3) Cu-MFI/AIE/473 K; (4) Cu-MFI/AIE/773 K; (5) Cu-MFI/VIE/773 K; (6) Cu-MFI/AIE/473 K partially reduced to 484 K; (7) Cu-MFI/VIE/473 K partially reduced to 533 K; (8) Cu-MFI/VIE/473 K.

The partial restoration of the 3610 cm^{-1} band for the Cu-MFI/AIE/473 K relative to Na-MFI indicates that zeolitic protons are reintroduced into the Na-MFI material by the $CuCl_2$ aqueous ion-exchange process, while the bands at 3737 cm^{-1}, 3692 cm^{-1}, and 3658 cm^{-1} indicate that the SiOH and AlOH species were not significantly affected. The 3590 cm^{-1} and 3575 cm^{-1} bands observed for the Na-MFI material are not present after the copper exchange, which is consistent with their assignment to water coordinated to sodium ions and replacement of sodium by copper in the exchange process. The broad band between 3600 cm^{-1} and 3300 cm^{-1} has been previously observed for copper ion-exchanged MFI and was attributed to water and hydroxide ions associated with Cu^{2+} ions (11). Cu-MFI/AIE/773 K shows significantly weaker bands at 3600 cm^{-1} to 3300 cm^{-1}, compared to Cu-MFI/AIE/473 K, in agreement with previous studies (11). Other bands in Cu-MFI/AIE/773 K are similar to those present in Cu-MFI/AIE/473 K. Partial reduction of the Cu-MFI/AIE/473 K at 483 K results in the formation of a broad band between 3600 cm^{-1} and 3300 cm^{-1}, possibly due to water produced by the reduction of copper hydroxides. The zeolitic proton peak at 3610 cm^{-1} does not appear to be significantly affected by the partial reduction process.

Cu-MFI/VIE/473 K possesses a silanol band at 3739 cm^{-1} and only a small band due to zeolitic protons at 3610 cm^{-1}. Two pronounced absorption regions are observed, one at 3448 cm^{-1} and another at 3360 cm^{-1}–3319 cm^{-1}. Similar peaks at 3440 cm^{-1} and 3350 cm^{-1} have been observed for "excessively" ion-exchanged copper mordenite (3, 4). The latter absorption peak was attributed to bridged OH groups coordinated between two Cu^{2+} ions (3, 4). The former peak was assigned to water coordinated to the copper ions in a copper hydroxyl dimer (3, 4). The occurrence of several peaks in the 3360 cm^{-1} to 3319 cm^{-1} region may be due to the multiple crystallographic locations in the zeolite in which the Cu^{2+} ions can reside. Partial reduction to 533 K of Cu-MFI/VIE/473 K results in the elimination of the bands which appear to be associated with a copper hydroxyl dimer. The 3610 cm^{-1} acidic proton band is not restored by the partial reduction. Cu-MFI/VIE/773 K shows no bands that could be associated with the copper hydroxyl dimer peaks or significant protons.

The spectra of materials after CO adsorption is shown in Fig. 11. Neither the H-MFI nor the Cu_2O/H-MFI materials show any significant CO absorption bands. In agreement with the microbalance results, Cu-MFI/AIE/473 K shows some absorbance, with peaks at approximately 2175 cm^{-1}

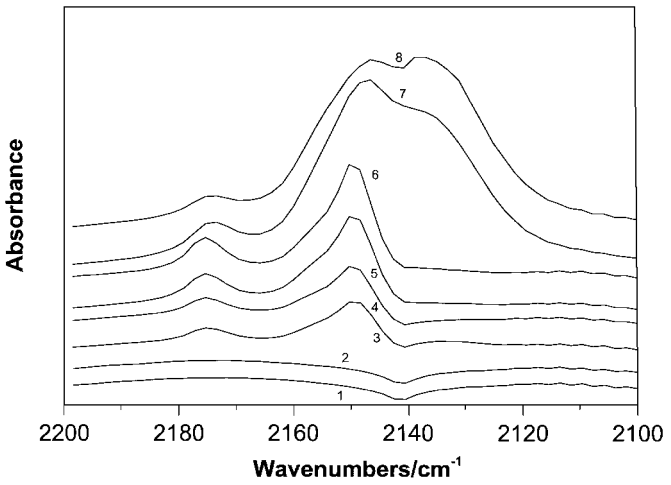

FIG. 11. IR CO adsorption results: (1) H-MFI/473 K; (2) Cu_2O/H-MFI/473 K; (3) Cu-MFI/VIE/473 K; (4) Cu-MFI/AIE/473 K; (5) Cu-MFI/AIE/773 K; (6) Cu-MFI/AIE/473 K partially reduced to 484 K; (7) Cu-MFI/VIE/773 K; (8) Cu-MFI/VIE/473 K partially reduced to 533 K.

and 2150 cm^{-1}. Previous investigations indicated that some of the Cu^+ ions in MFI can interact with CO to form $[Cu(CO)_2]^+$ ions with absorption peaks at 2177.5 cm^{-1} and 2151 cm^{-1} (10). The absorption attributable to adsorbed CO increases for the Cu-MFI/AIE/773 K relative to Cu-MFI/AIE/473 K, and partial hydrogen reduction of the Cu-MFI/AIE/473 K also results in an increase in these absorption bands. Cu-MFI/VIE/473 K also shows some adsorbed CO absorption bands, which is consistent with the microbalance results indicating that some CO is adsorbed on this material. Cu-MFI/VIE/773 K gives a significant increase in the absorption bands associated with the $[Cu(CO)_2]^+$ ions relative to Cu-MFI/VIE/473 K. An absorption band at 2137 cm^{-1} is also present, which is not normally observed for MFI samples with low copper concentrations and has been attributed to CO adsorbed on associated Cu^+ ions (10). Partial reduction to 533 K of Cu-MFI/VIE/473 K also produces similar bands with absorption intensities that are somewhat greater than that of the Cu-MFI/VIE/773 K.

DISCUSSION

Cu-MFI/VIE/473 K and Cu-BEA/VIE/473 K give rise to similar H_2 TPR spectra that consist of a low temperature band at 490 K and a high temperature band at about 610 K. These individual bands in each material have similar areas. This result is consistent with the reduction of Cu^{2+} ions to Cu^+ ions in the first peak and Cu^+ ions to copper metal for the second, and we expect Cu^{2+} ions to be present in the VIE materials because of the oxidation step after the CuCl vapor exchange, which was performed in order to eliminate disproportionation of the Cu^+ ions caused by exposure to humid air. The stepwise reduction of Cu^{2+} ions in hydrogen has been previously reported (11, 14, 23–27). The relatively small amounts of CO adsorbed on Cu-MFI/VIE/473 K and Cu-BEA/VIE/473 K as observed via microbalance and IR is also consistent with most of the copper ions being in the +2 oxidation state under these conditions, since Cu^{2+} ions do not strongly adsorb CO (10, 11, 22). Partial hydrogen reduction of Cu-MFI/VIE/473 K to 533 K (which corresponds approximately to the maximum of the first TPR peak of Cu-MFI/VIE/473 K) results in a considerable increase in the CO adsorption capacity which is also consistent with Cu^{2+} to Cu^+ reduction, since zeolite-coordinated Cu^+ ions have been shown to strongly adsorb CO (10–12, 18, 22, 28, 29). The IR bands at 2175 cm^{-1}, 2146 cm^{-1}, and 2137 cm^{-1} which are observed when CO is adsorbed on partially reduced Cu-MFI/VIE/473 K are also consistent with the presence of a significant quantities of zeolite-bound Cu^+ ions (10).

The mass to charge ratios of 18.6 and 16.1 for the first and second reduction peaks for the Cu-MFI/VIE/473 K and the mass to charge ratios of 19.5 and 14.4 Cu-BEA/VIE/473 K are consistent with the loss of a coordinated water or a hydroxide group for each reduction step. Further, the IR data for Cu-MFI/VIE/473 K shows OH bands previously attributed to bridging copper hydroxyl dimers and water coordinated to them (3, 4). Oxygen bridges between copper atoms have also been observed in copper exchanged mordenite by single crystal X-ray diffraction experiments (30). These results suggest that most of the copper atoms in Cu-MFI/VIE/473 K and Cu-BEA/VIE/473 K (recalling again that these materials are treated in O_2 after the CuCl exchange) exist as dimers like those shown in Fig. 12a, which are similar to dimers proposed by Kuroda *et al.* (3, 4). Since it is unlikely that all of the copper hydroxyl species are sufficiently close to form dimers, isolated copper hydroxyl ions like in Fig. 12b are likely present as well. The reduction of these isolated copper hydroxyl species may be the origin of the shoulder at 463 K observed in the hydrogen TPR spectrum for the CuCl vapor ion-exchange materials. The number of hydrogen atoms consumed by Cu-MFI/VIE/473 K material in both the first and second peak is fairly close to the number of protons present in the zeolite, suggesting that nearly all of the zeolite ion exchange sites are occupied by

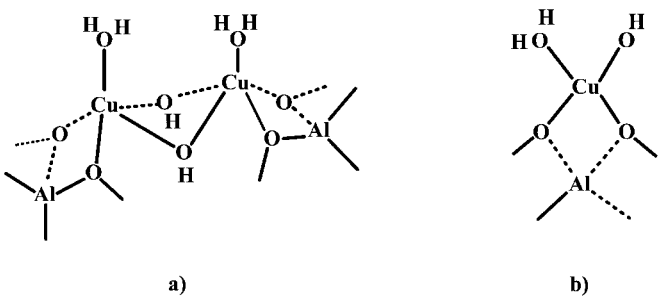

FIG. 12. Copper hydroxyl dimer (a) and monomer (b).

one copper ion, and is also consistent with the weakness of the 3610 cm^{-1} IR band associated with zeolitic protons. The amount of hydrogen consumed by the reduction of copper in Cu-BEA/VIE/473 K material is less than the initial number of protons in the H-BEA base, which may be the result of dealumination of the zeolite by the high temperatures and also the presence of HCl which is the product of the vapor ion-exchange process. The loss of crystallinity of this material relative to the H-BEA material as indicated by X-ray diffraction also supports this suggestion.

The results presented are consistent with the hydrogen reduction of copper hydroxyl ions and copper hydroxyl dimers to $(Cu\text{-}H_2O)^+Z^-$, where Z^- represents an anionic zeolite site. The second TPR reduction peak corresponds to reduction of these species to Cu^0 and H^+Z^-. The weight loss is likely due to loss of the coordinated water molecule.

When Cu-MFI/VIE and Cu-MFI/VIE are pretreated in vacuum or an inert atmosphere at 773 K instead of 473 K, we believe that restoration of Cu^+ occurs. The relative decrease in the amount of hydrogen consumed during reduction which occurs upon pretreatment of Cu-MFI/VIE and Cu-BEA/VIE to 773 K rather than 473 K is consistent with the thermal reduction of the Cu^{2+} ions to Cu^+ ions by this treatment. The 2175 cm^{-1}, 2146 cm^{-1}, and 2137 cm^{-1} IR bands present after exposure of the Cu-MFI/VIE/773 K to CO is also consistent with this hypothesis. Both Cu-MFI/VIE/773 K and Cu-BEA/VIE/773 K possess weight loss peaks on reduction at approximately 602 K. Heating the Cu-MFI/VIE/773 K in CO to 773 K does not significantly affect this weight loss peak. The general assumption that oxygen containing copper species are reduced by heating in CO (25) suggests that the weight loss peak is not due to loss of oxygen and is probably due to reduction of small amounts of $Z^-[CuCl]^+$ ions produced by reaction of the zeolite with the residual CuCl which was observed by XRD.

The reaction pathway leading to the formation of the copper hydroxyl ions and dimers in the CuCl VIE materials likely proceeds through several steps. Previous investigations have shown that CuCl vapor reacts with zeolitic protons to form HCl and Cu^+ ions coordinated to zeolite ion exchange sites (31–33), which we also expect in the first step of the formation process for the VIE materials. In the second step, which is oxidation at 373 K, we expect that $[Cu\text{-}O\text{-}Cu]^{2+}$ oxonium ions are formed, because previous reports (19, 34, 35) have shown that this reaction occurs. Other investigations have demonstrated that $[Cu\text{-}O\text{-}Cu]^{2+}$ ions can react with water to form $[Cu(OH)]^+$ ions (20) which we expect happens when the catalyst is removed from the furnace and exposed to humid air in the final step of the formation process. The unique feature of these materials is that they can be taken off the shelf and converted back to materials with a very high Cu^+ ion content by simple treatment in vacuum or an inert atmosphere at 773 K.

Cu-BEA/AIE/473 K behaves similar to Cu-BEA/VIE/473 K, only with a lower overall copper concentration. The similar hydrogen consumption of the first and second TPR peaks and the mass to charge ratios suggest that this material is also composed predominantly of copper hydroxyl ions and dimers. As with the CuCl vapor ion-exchange materials, these ions thermally reduce to Cu^+ ions on heating to 773 K. $[Cu(OH)]^+$ ions have also been previously proposed to be the major copper species present in ion-exchanged zeolites (14, 17, 19, 24, 27, 36, 37). The copper hydroxyl ions in this material possibly stem from reaction of the Cu^{2+} ions exchanged into the zeolite with H_2O to form zeolitic protons and $[Cu(OH)]^+$ ions (21, 25, 27).

The Cu-MFI/AIE/473 K is more complicated than the other materials. The hydrogen consumption corresponding to the low temperature TPR peak is significantly less than that of the second. Further, two weight loss peaks are observed in the high temperature region and the mass to charge ratio of the reduction region, 9.31, is much less than the ratios of 14.4–19.6 which we have attributed to the loss of coordinated water and hydroxyl groups for the other materials. Previous investigations have indicated that thermal reduction of Cu^{2+} ions in aqueous ion-exchanged MFI begins at temperatures slightly greater than 373 K (11, 12). The reduction temperature of the first high temperature peak observed on the microbalance, 589 K, is fairly close to the reduction temperature of Cu_2O, 602 K. Further, if Cu_2O were present and the O atom was lost as water on reduction, the expected mass to charge ratio of 8 could account for this observed mass to charge ratio.

Previous investigations have indicated that during the thermal reduction of Cu^{2+} ions to Cu^+ ions in Cu^{2+} ion-exchanged MFI, the EPR signal associated with zeolite coordinated Cu^{2+} ions disappears prior to the formation of photoluminescence bands associated with zeolite coordinated Cu^+ ions (9). These results and the results published in this paper are consistent with the thermal reduction of at least some $[Cu(OH)]^+$ ions to Cu_2O, oxygen, water, and zeolitic protons in Cu-MFI/AIE/473 K. Oxygen desorption from ion-exchanged Cu-MFI materials during heating has been previously reported (11, 18). The Cu_2O, which is not found in Cu-MFI/AIE/773 K, may react with zeolitic protons to form zeolite coordinated Cu^+ ions and water. The lower stability of the $[Cu(OH)]^+$ ions in MFI relative to BEA may be due to the lower pore volume of MFI and the absence of significant reduction of $[Cu(OH)]^+$ to Cu_2O in the Cu-MFI/VIE material may be due to the greater stability of the dimer (Fig. 12a) with respect to the isolated copper hydroxyl ions (Fig. 12b).

Previous reports have suggested that under the reaction conditions used for the 1-propanamine conversion, the Cu^+ ions are reduced to copper metal and zeolite acid sites (2). The acidic sites were postulated to catalyze the condensation of the 1-propanamine to dipropanamine and ammonia,

and the copper metal acts as a mild dehydrogenation catalyst that selectively removes the hydrogen atoms attached to the nitrogen and adjacent carbon. The results in this paper are consistent with those findings. For both the MFI and BEA materials the amount of imine formed increases with increasing copper loadings. Further, the maxima in the dipropanamine partial pressure curves observed for the Cu-MFI/VIE and Cu-BEA/VIE are consistent with the conversion of dipropanamine to the imine by dehydrogenation.

CONCLUSIONS

A process has been developed for exchanging one copper atom per zeolite ion-exchange site via CuCl vapor ion-exchange followed by oxidation to convert the copper to a form stable in humid air. These ions exist in the form of copper hydroxyl and copper hydroxyl dimers which are stable in air. The Cu^{2+} ions can be reduced to Cu^{1+} ions by either thermal treatment in an inert atmosphere or partial hydrogen reduction. Catalytic reactions of copper zeolites with a 1-propanamine reactant induces the reduction of the copper ions to dispersed copper metal and regenerates the zeolite acid sites, resulting in a bifunctional catalyst. The zeolite acid sites selectively dimerize 1-propanamine to dipropanamine and the dispersed copper metal dehydrogenates the dipropanamine to 1-propanamine, N-(1-propylidene) by the selective removal of the hydrogen atoms attached to the nitrogen and adjacent carbon.

ACKNOWLEDGMENTS

The authors gratefully acknowledge the financial support of the National Science Foundation Grant CTS-9634754.

REFERENCES

1. Kanazirev, V. I., Price, G. L., and Dooley, K. M., *J. Catal.* **148**, 164 (1994).
2. Guidry, T. F., and Price, G. L., *in* "Catalysis of Organic Reactions" (F. E. Herkes, Ed.), Marcel Dekker, New York, pp. 601–606 (1998).
3. Kuroda, Y., Kotani, A., Maeda, H., Moriwaki, H., Morimato, T., and Nagao, M., *J. Chem. Soc. Faraday Trans.* **88**, 1583 (1992).
4. Kuroda, Y., Kotani, A., Uemura, A., Yoshikawa, Y., and Morimato, T., *J. Chem. Soc. Chem. Commun.*, 1631 (1989).
5. Price, G. L., and Kanazirev, V., *Zeolites* **18**, 33 (1997).
6. Kanazirev, V., Dooley, K. M., and Price, G. L., *J. Catal.* **146**, 228 (1994).
7. Shyr, Y. N., and Price, G. L., *Ind. Eng. Chem. Prod. Res. Des.* **23**, 536 (1984).
8. Corma, A., Palomeres, A., and Marques, F., *J. Catal.* **170**, 132 (1997).
9. Wichterlova, B., Dedecek, J., Sobalik, Z., Vondrova, A., and Klier, K., *J. Catal.* **169**, 194 (1997).
10. Hadjiivanov, K. I., Kantcheva, M. M., and Klissurski, D. G., *J. Chem. Soc. Faraday Trans.* **92**, 4595 (1996).
11. Anpo, M., Matsuoka, M., Shioya, Y., Yamashita, H., Giamello, E., Morterra, C., Che, M., Patterson, H., Webber, S., Ouellette, S., and Fox, M. A., *J. Phys. Chem.* **98**, 5744 (1994).
12. Yamashita, H., Matsuoka, M., Tsuji, K., Shioya, Y., Anpo, M., and Che, M., *J. Phys. Chem.* **100**, 397 (1996).
13. Connerton, J., Joyner, R. W., and Padley, M. B., *J. Chem. Soc. Faraday Trans.* **91**, 1841 (1995).
14. Dedecek, J., and Wichterlova, B., *J. Phys. Chem.* **98**, 572 (1994).
15. Giamello, E., Murphy, D., Magnacca, G., Morterra, C., Shioya, Y., Normura, T., and Anpo, M., *J. Catal.* **136**, 510 (1992).
16. Grunert, W., Hayes, N. W., Joyner, R. W., Shpiro, E. S., Siddiqui, M. R. H., and Baeva, G. N., *J. Phys. Chem.* **98**, 10832 (1994).
17. Larsen, S. C., Aylor, A., Bell, A. T., and Reimer, J. A., *J. Phys. Chem.* **98**, 11533 (1994).
18. Jacobs, P. A., Wilde, W., Schoonheydt, R. A., Uytterhoeven, J., and Beyer, H., *J. Chem. Soc. Faraday I* **72**, 1221 (1976).
19. Valyon, J., and Hall, W. K., *J. Catal.* **143**, 520 (1993).
20. Vaylon, J., and Hall, W. K., *J. Phys. Chem.* **97**, 7054 (1993).
21. Ward, J. W., *Trans. Faraday Soc.* **67**, 1489 (1971).
22. Sarkany, J., and Sachtler, W. M. H., *Zeolites* **14**, 7 (1994).
23. Texter, J., Strome, D. H., Herman, R. G., and Klier, K., *J. Phys. Chem.* **81**, 333 (1977).
24. Wichterlova, B., Dedeck, J., and Vondrova, A., *J. Phys. Chem.* **99**, 1065 (1995).
25. Beutel, T., Sarkany, J., Lei, G. D., Yan, J. Y., and Sachtler, W. M. H., *J. Phys. Chem.* **100**, 845 (1996).
26. Yan, J. Y., Lei, G. D., Sachtler, W. M. H., and Kung, H. H., *J. Catal.* **161**, 43 (1996).
27. Petunchi, J. O., Marcelin, G., and Hall, W. K., *J. Phys. Chem.* **96**, 9967 (1992).
28. Borovokov, V. Y., and Karge, H. G., *J. Chem. Soc. Faraday Trans.* **91**, 2035 (1995).
29. Huang, Y., *J. Catal.* **30**, 187 (1973).
30. Attfield, M. P., Weigel, S. J., and Cheetham, A. K., *J. Catal.* **170**, 227 (1997).
31. Szanyi, J., and Paffett, M. T., *J. Catal.* **164**, 232 (1996).
32. Spoto, G., Bordiga, S., Ricchiardi, G., Scarano, D., Zecchina, A., and Geobaldo, F., *J. Chem. Soc. Faraday Trans.* **91**, 3285 (1995).
33. Lamberti, C., Bordiga, S., Savalggio, M., Spoto, G., Zecchina, A., Geobaldo, F., Vlaic, G., and Bellatreccia, M., *J. Phys. Chem. B* **101**, 344 (1997).
34. Li, Y., and Hall, W. K., *J. Catal.* **129**, 202 (1991).
35. Jacobs, P. A., Tielen, M., Linart, J., Uytterhoevan, J. B., and Beyer, H., *J. Chem. Soc. Faraday I* **72**, 2793 (1976).
36. Blint, R. J., *J. Phys. Chem.* **100**, 19518 (1996).
37. Trout, B. L., Chakraborty, A. K., and Bell, A. T., *J. Phys. Chem.* **100**, 17582 (1996).